RESEARCH PAPER

Network Pharmacology and Molecular Dynamics reveal FXR and OATP1B1 mediated Anti-Cholestatic Potential of Hesperidin

Faiz Ahmed Kazi[1], Namit Kudatarkar[1]*, Vishal S Patil[1], Shamanand P Mallapur[1], Mohammed Zaid Bepari[1]

[1]Department of Pharmacology, KLE College of Pharmacy, Belagavi, KLE Academy of Higher Education and Research, Deemed-to-be-University, Belagavi 590010, India.

ABSTRACT

Drug-induced cholestasis (DIC) is a subtype of drug-induced liver injury (DILI) that causes hepatocellular damage, oxidative stress, bile acid accumulation, and inflammation. The present study uses an integrated in silico method which combines network pharmacology (NP), protein-protein interaction (PPI), molecular docking (MDK), and molecular dynamics (MD) simulations to examine the hepatoprotective potential of hesperidin (HSP), a bioactive flavonoid. Forty-one of the 105 hesperidin-associated genes identified through target prediction were similar with DIC-related targets, suggesting a significant mechanistic relation. Key roles in oxidative stress, bile acid metabolism, and inflammatory signalling pathways, such as farnesoid X receptor (FXR) signalling along with transporter regulation, were identified by enrichment analysis. MDK revealed significant binding affinity of hesperidin toward FXR (-9.5 kcal/mol) and organic anion transporting polypeptide 1B1 (OATP1B1) (-7.9 kcal/mol), with stable hydrogen bonding and hydrophobic interactions during 100 ns MD simulations ensured structural stability and sustained ligand–protein interactions. Drug-likeness and toxicity assessments suggested a favourable safety profile, with non-mutagenic and non-carcinogenic profile for hesperidin. In conclusion, hesperidin modulates oxidative stress, inflammation, and bile acid homeostasis in DIC, suggesting multi-target regulatory potential that supports its development as a promising hepatoprotective agent.

Keywords: Hesperidin, drug-induced cholestasis, molecular docking, bile acid transporters, FXR signalling.

How to cite this article: Kazi FA, Kudatarkar N, Patil VS, Mallapur SP, Bepari MZ. Network Pharmacology and Molecular Dynamics reveal FXR and OATP1B1 mediated Anti-Cholestatic Potential of Hesperidin. Int J Drug Deliv Technol. 2026;16(64s):411-427. DOI: 10.25258/ijddt.16.64s.41

Source of support: Nil

Conflict of interest: None

INTRODUCTION

Cholestasis is a pathological condition that occurs due to impaired bile production or reduced bile flow from hepatocytes to the duodenum [1]. Oxidative stress, hepatocyte necrosis or apoptosis, mitochondrial dysfunction, and progressive cirrhosis or fibrosis can all result from continuous bile retention [2]. Either obstruction of the extrahepatic biliary tract, or intrahepatic disorders (hepatocellular dysfunction, transporter failure) can lead to cholestasis [3].

A type of drug-induced liver injury (DILI), drug-induced cholestasis (DIC) accounts for 8–56% of reported DILI cases, depending upon the population and diagnostic standards applied [4]. Examples of such drugs include antibiotics, NSAIDs, statins, drugs for psychiatric disorders, and chemotherapeutics, all of which disrupts bile acid homeostasis by activating inflammatory signalling pathways or altering transporter function (e.g., BSEP, NTCP, MRP2). Moreover, herbal supplements sometimes potentiate cholestasis, complicating diagnosis and treatment [5].

At the molecular level, bile acid homeostasis is regulated by hepatocellular uptake and efflux transporters, including Sodium Taurocholate Co-Transporting Polypeptide (NTCP), Organic Anion Transporting Polypeptide 1B1 (OATP1B1), Bile Salt Export Pump (BSEP), and Multidrug Resistance-associated Protein 2 (MRP2) together with nuclear receptors such as farnesoid X receptor (FXR) and small heterodimer partner (SHP) [6,7].

FXR plays a central role in the regulation of transport, detoxification, and bile acid synthesis. By downregulating cholesterol 7α-hydroxylase (CYP7A1), activation of FXR suppresses bile acid synthesis while simultaneously promoting bile acid export through the induction of BSEP expression. Impairments in these pathways lead to the accumulation of toxic bile acids causing damage to hepatocytes [8,9].

Despite advances in hepatology, DIC is still treated without any specific therapeutic intervention. Current practice in therapy includes stopping the harmful drug and giving treatment with drugs like cholestyramine, ursodeoxycholic acid (UDCA), or N-acetylcysteine

(NAC). However, these treatments may have adverse side effects and may not give good biochemical response. New, safe, and effective hepatoprotective medications are thus required [10–12].

Flavonoids show promise in liver protection by mitigating oxidative stress and inflammation; among them, hesperidin (HSP; 3,5,7-trihydroxyflavanone-7-rhamnoglucoside), a widely available flavanone glycoside (vitamin P), possesses well-documented anti-inflammatory, analgesic, and antioxidant activities [13-15]. The acute oral toxicity study shows HSP to have an LD50 of >2000 mg/kg (4837.5 mg/kg) [16]. Experimental studies have suggested that hesperidin can modulate oxidative stress, inflammatory signaling pathways, and bile acid metabolism. However, a coordinated multi-target mechanistic role remains insufficiently characterized [17].

A systems-level framework for describing the complex relationships between bioactive substances, molecular targets, and pathways linked to disease is provided by network pharmacology (NP) [18]. By combining molecular docking (MDK) with molecular dynamics (MD) simulations, the method allows for the generation of mechanistic hypotheses and validates target prediction through structural and dynamic evaluation. The in-silico integrative strategies are particularly suited for multi-target natural products which treat complex diseases like cholestasis [19].

The present study aims to elucidate the molecular pathways through which HSP protects against DIC by using an integrated in-silico approach combining NP, MDK, and MD simulations. The research establishes a scientific basis for developing HSP as a multi-target drug treatment for cholestatic liver diseases.

MATERIALS AND METHODS

2.1 Compound Selection, Target Identification of HSP and DIC

Hesperidin (HSP; PubChem CID: 10621) was selected for this study based on its reported hepatoprotective, antioxidant, and anti-inflammatory activities [17,20]. The three-dimensional structure of HSP was obtained from the PubChem (https://pubchem.ncbi.nlm.nih.gov/ Retrieved on September 22, 2025), and the canonical SMILES and Structure Data File (SDF) formats were downloaded for subsequent molecular docking and network pharmacology analyses [21]. Potential molecular targets were identified using the Comparative Toxicogenomics Database (CTD) (https://ctdbase.org/ Retrieved on September 23, 2025) by querying "hesperidin." After removing duplicate and irrelevant entries, the curated target dataset was used for network pharmacology, functional enrichment, and molecular docking studies. DIC-associated genes were retrieved from the GeneCards database (https://www.genecards.org/ Retrieved on September 24, 2025) using the keyword "drug-induced cholestasis," with the search restricted to *Homo sapiens* [22,23]. Genes with a relevance score ≥30 were retained to ensure reliability. After standardization and removal of duplicate entries, the curated DIC gene set was compared with HSP-related targets to identify overlapping genes. Common targets were determined using Venny 2.1.0 and subsequently employed for network pharmacology and computational analyses.

Table 1. HSP predicted for FXR activation assay

Compound	PC ID	Molecular Formula	Experimental Assay	Reference Compound PC ID	Reference
HSP	10621	$C_{28}H_{34}O_{15}$	FXR activation assay; hepatoprotective activity in HepaRG cells, and ANIT-induced cholestasis in mice	447715 (Obeticholic acid)	[17]

PubChem ID; ANIT: Alpha-naphthylisothiocyanate

2.2 Gene Set Enrichment Analysis and Network Construction

Functional enrichment and protein–protein interaction (PPI) analyses of the common HSP–DIC targets were performed using the STRING database (version 12.0; https://string-db.org/ Retrieved on September 25, 2025), with the analysis restricted to *Homo sapiens* [23,24]. Pathway enrichment was subsequently conducted using the KEGG database (https://www.kegg.jp/kegg/pathway.html Retrieved on September 29, 2025) to identify biological pathways associated with the shared targets. Statistical significance was determined using a false discovery rate (FDR) threshold of ≤0.05. Pathways involved in oxidative stress, inflammatory signalling, and bile acid metabolism were prioritized for mechanistic interpretation. A compound–target–pathway network was constructed in Cytoscape (v3.7.2) to visualize interactions among HSP, target proteins, and enriched pathways. Nodes represented the compound, proteins, and pathways, whereas edges denoted their interactions. To identify key regulatory targets, network topology was

evaluated using the NetworkAnalyzer plugin, focusing on degree, betweenness, and closeness centrality parameters [25].

2.3 Molecular Docking

2.3.1 Preparation of Ligand

PubChem (https://pubchem.ncbi.nlm.nih.gov/ Retrieved on October 9, 2025) provided the 3D structure of HSP in SDF format and it was prepared for MDK analysis using PyRx with the integrated AutoDock Vina interface. The MMFF94 force field was used to minimize the energy of the ligand structure prior to docking with the objective to remove steric conflicts and achieve a stable conformation. After adding polar hydrogen atoms, the ligand was provided with Gasteiger partial charges. The Open Babel module included with PyRx was then used to transform the optimized structure into PDBQT format. The HSP conformer with the lowest energy was chosen as the ligand structure for docking simulations. To provide flexible ligand docking inside the target protein binding sites, rotatable bonds were generated by software during PDBQT conversion [26–28].

2.3.2 Preparation of Protein

The Research Collaboratory for Structural Bioinformatics (RCSB) Protein Data Bank (https://www.rcsb.org/ Retrieved on October 16, 2025) provided the target protein's 3D structures. For the docking studies, crystal structures of the OATP1B1 (PDB ID: 8HNC) and FXR (PDB ID: 3BEJ) were used [29]. The GalaxySite server (https://galaxy.seoklab.org/ Retrieved on October 16, 2025) was used to preprocess protein structures in order to eliminate heteroatoms, co-crystallized ligands, and crystallographic water molecules. Following the addition of polar hydrogen atoms, AutoDock Tools was used to assign Gasteiger charges. The PROCHECK and ERRAT modules, which are accessible via the SAVES website (https://saves.mbi.ucla.edu/ Retrieved on October 17, 2025) (https://saves.mbi.ucla.edu/ Retrieved on October 18, 2025) were used to validate the constructed protein models in order to assure structural stability. The processed protein structures were transformed into PDBQT format for MDK studies after validation. The appropriate protein chain containing the ligand-binding domain was selected for docking [21].

2.3.3 Assessing Active Site Residues

Based on the ligand-binding areas found in the co-crystallized structures of FXR (3BEJ) and OATP1B1 (8HNC) acquired from the RCSB Protein Data Bank, the active-site residues of the target proteins were determined. The PrankWeb server (https://prankweb.cz/ Retrieved on October 19, 2025) was utilized to estimate likely binding pockets and druggable locations within the protein structures to better describe potential ligand-binding areas [30].

2.3.4 Protein-Receptor Docking

HSP's binding affinity to the target proteins FXR (3BEJ) and OATP1B1 (8HNC) was assessed by MDK using the AutoDock Vina inside PyRx. The anticipated active binding sites found during the development of proteins and binding pocket analysis were used to build docking grids [25]. The resulting receptor structures were archived in PDBQT format for docking analysis after crystallographic water molecules and heteroatoms were eliminated and Gasteiger charges were assigned. The grid box centre for FXR (3BEJ) was set at X = 12.52, Y = 19.28, and Z = 28.53 and its dimensions were 48.91 × 51.35 × 49.71 Å. For OATP1B1 (8HNC), the box dimensions were 97.79 × 51.91 × 70.33 Å , and the grid centre was set up at X = 102.50, Y = 109.33, and Z = 105.95. [21]. Docking was carried out using an exhaustiveness value of 8. The conformations with the lowest binding energies were chosen for further interaction analysis, and binding affinities for each docking posture were reported in kcal/mol. Discovery Studio Visualizer 2019 was used to further evaluate and show protein-ligand interactions, including hydrophobic contacts and hydrogen bonding [31].

2.4 MD Simulation

Schrödinger Desmond software for 100 ns MD simulations was used to evaluate the stability of protein-ligand interactions. In a cubic box with 10 Å 10 Å 10 Å periodic borders, systems were solvated using the simple point charge (SPC) water model, neutralized using Na^+/Cl^- counter-ions, and then restricted using the SHAKE algorithm. The particle mesh Ewald approach was used to tackle long-range electrostatics, using a Lennard-Jones cutoff of 10.0 Å. The system was equilibrated by means of standard procedure. Finally, Construction runs were conducted utilizing a Nosé-Hoover chain thermostat (1.0 ps) and a Martyna-Tobias-Klein barostat (2.0 ps) at 300 K and 1.01325 bar following conventional equilibration, respectively, with a Coulombic short-range cutoff radius of 9.0 Å" [32,33]. Root-mean-square deviation (RMSD), root-mean-square fluctuation (RMSF), and radius of gyration (rGyr) were studied to determine residue-wise fluctuations to assess structural stability and dynamics.

2.5 Drug-Likeness and Toxicity Prediction

HSP's physicochemical characteristics and drug-likeness were assessed using Lipinski's Rule of Five criteria, which include molecular weight, hydrogen bond donors, hydrogen bond acceptors, and logP value. The MolSoft online server (https://www.molsoft.com/ accessed on September 28, 2025) was used to forecast these characteristics and to determine the compound's drug-likeness score (DLS) [20,21,34]. The ADVERpred web server was used to evaluate possible adverse drugs reactions [35,36]. The PreADMET server (https://preadmet.webservice.bmdrc.org/introduction/ accessed on September 29, 2025) predicted toxicological properties which included Ames mutagenicity and carcinogenicity and hERG inhibition to assess the safety profile of HSP [37].

3 RESULTS

3.1 Identification of HSP Targets Relevant to DIC

HSP was selected as the active pharmaceutical molecule for the current research based on previously published experimental data showing hepatoprotective and antioxidant effects [17,20,38]. The CTD was used to identify 105 possible HSP-associated protein targets, along with genes associated with DIC reported in the literature. The 41 common targets identified by interaction analysis between the predicted HSP targets and DIC-associated suggest a connection between the pharmacological actions of HSP and the molecular mechanisms involved in cholestatic liver injury. MDK, NP, enrichment analysis, and MD studies were all based on these common targets. The FXR and OATP1B1 were given priority among these targets because of their established functions in the synthesis as well as transport of bile acids [17], as well as the availability of structural data appropriate for MDK and MD simulations.

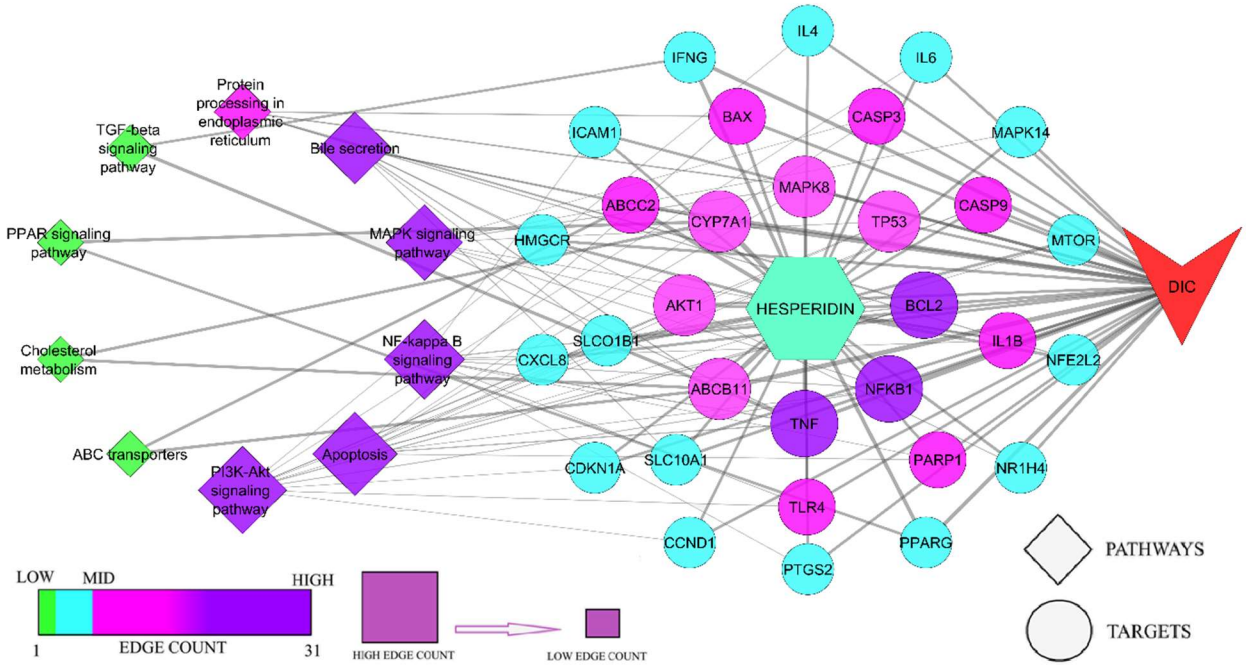

Figure 1. Network Representation of HSP-Target-Pathway.

3.2 Gene Sets Enrichment Analysis and Network Analysis

Among the 41 intersecting HSP-DIC targets, a functional enrichment analysis identified 163 significantly enriched pathways. 10 of these pathways had a direct connection to the DIC pathophysiology as shown in Figure 1. Out of 41 targets 31 were present in identified enriched pathways. The probable PPI interactions of the HSP regulated targets is shown in (Figure 2) Bile secretion, cholesterol metabolism, ABC transporter activity, apoptosis, oxidative stress-related pathways, and important signaling pathways like PI3K-Akt, MAPK, and NF-κB were among them [35,39]. Key regulators involved in bile acid production along with its transport, such as FXR (NR1H4), BSEP (ABCB11), NTCP (SLC10A1), OATP1B1 (SLCO1B1), MRP2 (ABCC2), CYP7A1, and HMGCR were enriched in the bile secretion and cholesterol metabolism pathways as shown in (Figure 1). Additionally, the complex nature of cholestatic liver injury was highlighted by the

enrichment of antioxidant defense genes like NFE2L2, PPARG, PARP1, and AKT1, as well as inflammatory mediators like TNF, IL6, IL1B. Moreover, a number of genes were linked to the control of cell cycle integrity. Network topology analysis using Cytoscape revealed FXR, OATP1B1, BSEP, and CYP7A1 as high-degree hub nodes.

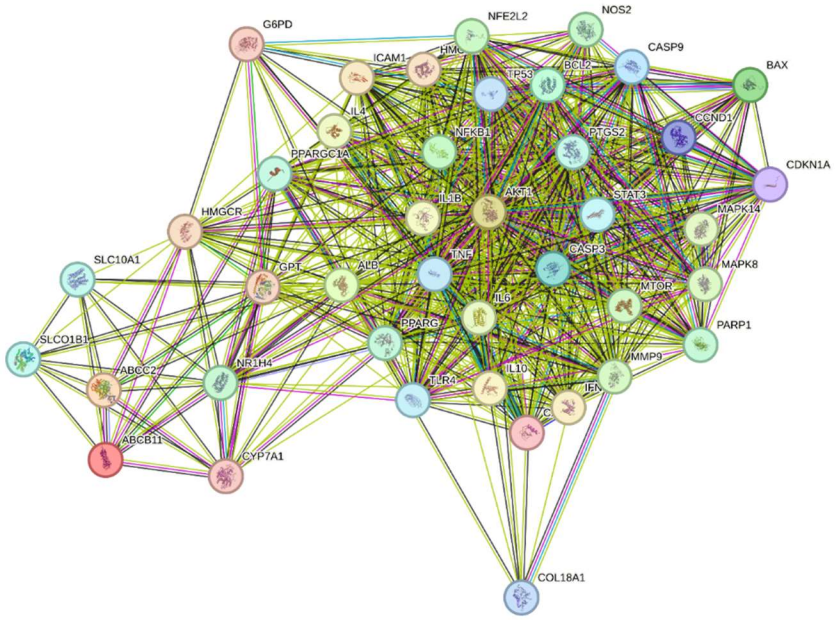

Figure 2. PPI of genes regulated by HSP.

3..3 Ligand-Protein Docking

The Ramachandran plot and ERRAT analyses were used to verify the structural quality of the chosen protein targets before molecular docking [40]. 91.8% of residues in the most favored regions of the FXR crystal structure (3BEJ) were found in additionally allowed regions, 7.0% in generously allowed regions, 0.7% in generously allowed regions, and only 0.5% in disallowed regions (Figure 3a). Excellent structural stability appropriate for docking studies was further confirmed by the ERRAT quality factor of 99.08% (Figure 3b). With 93.6% of residues in the most preferred regions and an ERRAT score of 91.60%, OATP1B1 (8HNC) also demonstrated high structural reliability (Figure 3c, d). Protein stability was unaffected by the minor variations found in 8HNC, which were linked to flexible loop regions.

Strong binding affinities of HSP toward FXR (3BEJ) and OATP1B1 (8HNC) were shown by docking analysis (Table 2). With a docking score of −9.5 kcal/mol against FXR, HSP formed seven hydrophobic interactions with Ala291, Leu287, Met290, and Ile335 and six hydrogen bond contacts with Lys338, Arg331, and His344 (Figure 4c). These interactions suggested that HSP was stablely accommodated in the FXR ligand-binding pocket. With hydrogen bond interactions involving His575, Glu185, Tyr352, and Thr357 as well as hydrophobic contacts formed by Ser576, Lys41, and Ile353, HSP demonstrated a docking score of −7.9 kcal/mol against OATP1B1, supporting stable ligand binding within the transporter cavity.

Table 2. Prioritized protein targets' binding affinities with HSP and UDCA

Ligand	PC ID	Target	BE (Kcal/ Mol)	Total No. of Interaction	NAS	HBI	NHBI
HSP	10621	3BEJ	-9.5	7	7	LYS 338 (2), ARG 331 (2), HIS 344 (2).	ALA 291 (2), LEU 287, MET

							290 (2), ILE 335 (2), ALA 291 (2).
		8HNC	-7.9	7	5	HIS 575, GLU 185, TYR 352, THR 357.	SER 576, LYS 41, ILE 353.
UDCA*	31401	3BEJ	-9.5	10	10	SER 332.	MET 265, LEU 287, MET 290, ALA 291, HIS 294, MET 328, ARG 331, ILE 352, HIS 447.
		8HNC	-7.8	7	7	ASN 213, SER 548.	VAL 189, VAL 349, TYR 352, PHE 386, HIS 555.

PC ID: PubChem ID; NAS: Number of Active Sites; HBI: hydrogen bond interactions; NHBI: Non-hydrogen bond interactions (Van Der Waals, Pi-Alkyl, Ch,Pi-Cation, Pi-Sigma, Pi-Pi Stacked, Pi-Pi T-Shaped Interactions); and BE: Binding Energy. It was emphasized how chemicals interacting with catalytic triad residues. *Known standards

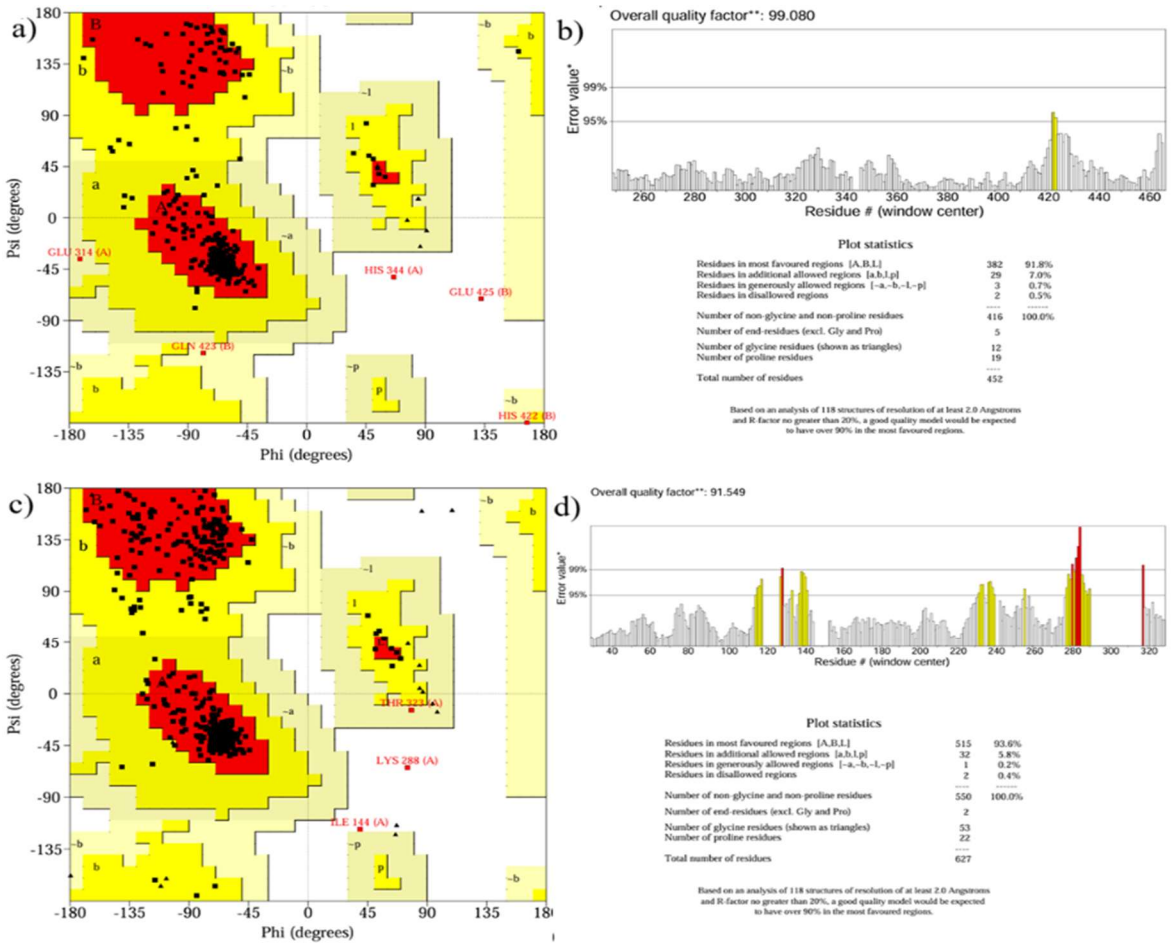

Figure 3. Features of PDB ID:3BEJ. (a) PROCHECK Ramachandran plot. (b) ERRAT's overall quality forecast. Features of PDB ID:8HNC. (c) PROCHECK Ramachandran plot. (d) ERRAT's overall quality forecast. * To show how confidently areas that surpass that error value may be rejected, two lines are displayed on the error axis. *Stated as the proportion of the protein for which the computed error value is less than the 95% rejection threshold.

3.3 Assessment of Active Site Residues

Based on ligand-binding data from the RCSB Protein Data Bank structures, the target proteins' active-site residues were determined. Key residues in the binding region of FXR (3BEJ) were Lys338, Arg331, His344, Ala291, Leu287, Met290, and Ile335. Similarly, His575, Ser576, Lys41, Glu185, Tyr352, Ile353, and Thr357 were found to be the active-site residues of OATP1B1 (8HNC) based on PDB structural data. The docking grid regions were identified by combining the computationally revealed binding-site residues from the PDB structures with the predicted pockets from PrankWeb and supporting literature evidence to precisely identify important binding regions for MDK studies.

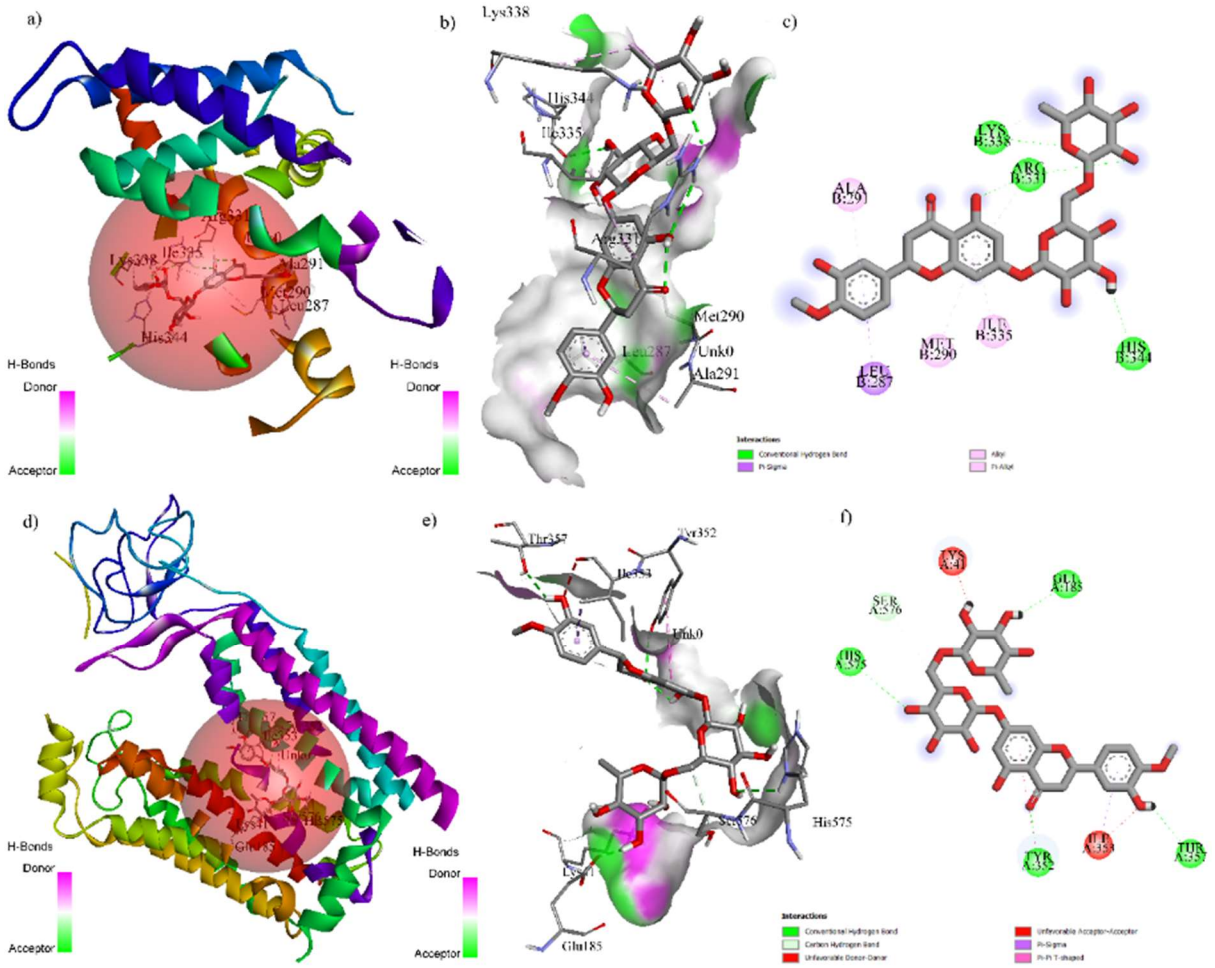

Figure 4. Intermolecular Interactions of HSP with FXR-3BEJ **(a)** HSP interaction at 3BEJ binding pocket; (b) 3D representation of HSP interaction with 3BEJ at its residue site; (c) 2D representation of Ligand-Protein Contacts LYS B:338, ARG B:331, HIS B:344. Intermolecular Interactions of HSP with OATPs-8HNC **(d)** HSP interaction at 8HNC binding pocket; (e) 3D representation of HSP interaction with 8HNC at its residue site; (f) 2D representation of Ligand-Protein Contacts HIS A:575, GLU A:185, TYR A352, THR A:357.

3.4 MD Simulation of DIC-Ligand Complexes

3.4.1 HSP-FXR Complex

To assess the HSP-FXR (3BEJ) complex's structural stability and binding stability, a 100 ns MD simulation was run [41]. Throughout the simulation, the protein backbone RMSD stayed between 1.4 and 2.8 Å, indicating that the FXR structure preserved conformational stability. HSP remained steadily situated inside the ligand-binding domain only showing minor conformational changes, according to the ligand RMSD, which varied from 2.0 to 3.5 Å when compared to the protein (FXR-5a). Higher fluctuations were mostly seen in terminal and loop regions far from the ligand, while RMSF analysis revealed restricted residue flexibility within the binding site (0.6-1.2 Å) (Figure 5b). Additionally, ligand molecular level RMSF values

were low (<1.0 Å), suggesting that HSP underwent little internal deformation during the simulation. The receptor's overall structural integrity was verified by the stability of the secondary structure element (SSE) profile, which maintained the α-helix and β-sheet content at roughly 62-65%. A constant number of hydrogen bonds with residues Gln263 (~29%) and Glu334 (~28-29%) were found through interaction analysis. Moreover, a dominant interaction involving the phenolic hydroxyl group persisted for roughly 98% of the simulation. Furthermore, Arg331, Leu287, Ile335, Met290, and Met328 were found to have stable hydrophobic interactions that helped maintain ligand retention in the binding pocket. Additionally, there was no structural unfolding or complex destabilization, as indicated by the rGyr, which stayed constant between 6.2 and 6.8 Å (Figure 5c; Table 3). HSP's function as a modulator of FXR-mediated signalling pathways related to DIC is supported by the MD results.

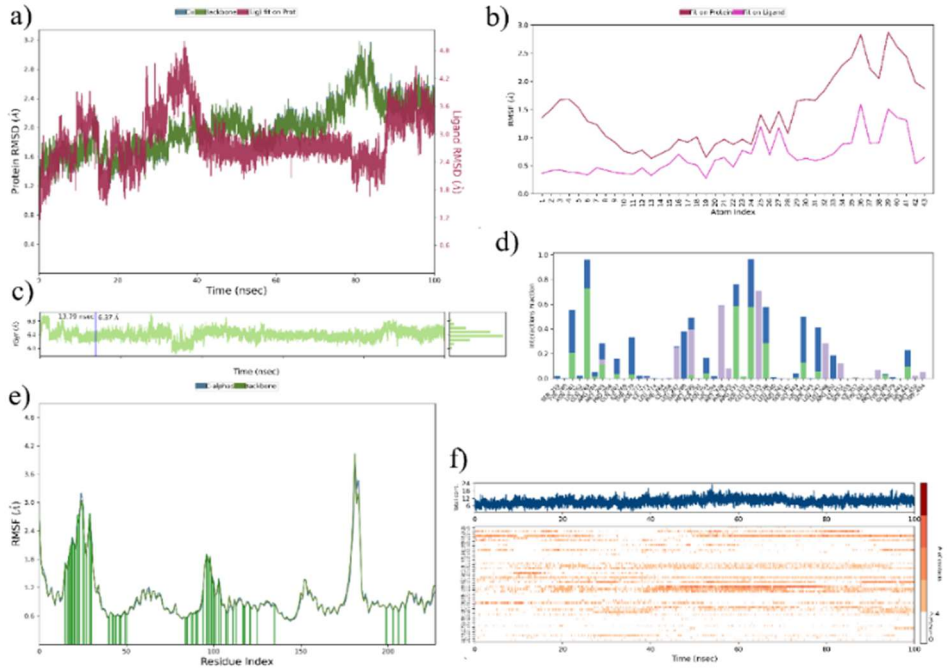

Figure 5. MD trajectories for a 100 ns simulation of HSP in combination with FXR (3BEJ) (a) RMSD, (b) RMSF, (c) rGyr, and (d-f) Ligand-protein contracts based on residues.

Table 3. HSP's interaction with protein targets following a 100 ns MD simulation

Ligand Name-Protein Complex	Amino Acid Residue	Ligand Atoms	Ligand Atoms Position	Ligand Atoms Interactions with Protein Residue (%)
HSP-3BEJ COMPLEX	GLN263	OH	18	29
HSP-3BEJ COMPLEX	GLU334	OH	44	28
HSP-3BEJ COMPLEX	ARG331	OH	47	43
HSP-3BEJ COMPLEX	ILE335	OH	65	29
HSP-3BEJ COMPLEX	LEU287	Aromatic / Hydrophobic	---	---
HSP-3BEJ COMPLEX	MET290	Aromatic / Hydrophobic	25-30	---
HSP-3BEJ COMPLEX	MET328	Aromatic / Hydrophobic	25-30	---

HSP-3BEJ COMPLEX	LEU348	Hydrophobic	---	---
HSP-8HNC COMPLEX	PHE38	OH	12	90+ (H-bond + hydrophobic)
HSP-8HNC COMPLEX	LYS41	OH	14	10-20.
HSP-8HNC COMPLEX	THR42	OH	16	15-25.
HSP-8HNC COMPLEX	ALA45	OH	18	5-10.
HSP-8HNC COMPLEX	ILE46	OH	20	20-30.
HSP-8HNC COMPLEX	GLU74	OH	22	10-15.
HSP-8HNC COMPLEX	ASN77	OH	24	10-15.
HSP-8HNC COMPLEX	VAL189	Aromatic / Hydrophobic	-	80+
HSP-8HNC COMPLEX	LEU209	Hydrophobic	-	30-40.
HSP-8HNC COMPLEX	ASN212	OH	28	15-25.
HSP-8HNC COMPLEX	ALA216	OH	30	35-40.
HSP-8HNC COMPLEX	MET217	Aromatic / Hydrophobic	-	10-20.
HSP-8HNC COMPLEX	THR345	OH	34	10-15.
HSP-8HNC COMPLEX	GLN348	OH	36	20-30
HSP-8HNC COMPLEX	TYR352	OH	40	Oct-18
HSP-8HNC COMPLEX	ILE353	Hydrophobic	-	12-20.
HSP-8HNC COMPLEX	THR357	OH	42	8-12.
HSP-8HNC COMPLEX	PHE360	Aromatic / π	-	10-15.
HSP-8HNC COMPLEX	LEU386	Hydrophobic	-	10-12.
HSP-8HNC COMPLEX	SER548	OH	44	15-18
HSP-8HNC COMPLEX	ILE579	Hydrophobic	-	8-10.
HSP-8HNC COMPLEX	ARG580	OH	46	12-15.

3.4.2 HSP-OATPs Complex

HSP's conformational stability and interaction persistence were assessed using a 100 ns MD simulation inside the binding domain of (OATP1B1; PDB ID: 8HNC). Throughout the simulation, the protein backbone RMSD remained constant between 2.0 and 4.2 Å, indicating that the transporter's overall structural integrity was preserved (Figure 6a). Because of its relatively large and flexible polyphenolic structure, HSP was able to remain accommodated within the binding pocket despite moderate positional adjustments, as indicated by the ligand RMSD, which ranged from 3.0 to 5.0 Å when calculated with respect to the protein. Most residues in the binding region had RMSF values between 0.8 and 1.6 Å (Figure 6b), indicating localized residue flexibility. In loop and peripheral areas far from the binding site, higher fluctuations were mainly seen. HSP's internal displacement during the simulation was limited, as indicated by ligand molecular level RMSF values that were less than 1.5 Å. Phe38, Lys41, Thr42, Ala45, Ile46, Glu74, Asn77, Val189, Leu209, Asn212, Ala216, Met217, Thr345, Leu348, Gln348, Tyr352, and Ile353 were among the important residues with which interaction fraction analysis revealed persistent

contacts. Hydrophobic contacts and hydrogen bonding were the main stabilizers of these interactions, which helped to maintain ligand retention inside the binding domain. For most of the 100 ns simulation, prolonged ligand-protein interactions were further verified by the contact timeline heatmap. Furthermore, there was no indication of complex destabilization or structural unfolding, and the rGyr stayed compact, varying between 5.3 and 6.4 Å (Figure 6c; Table 3).

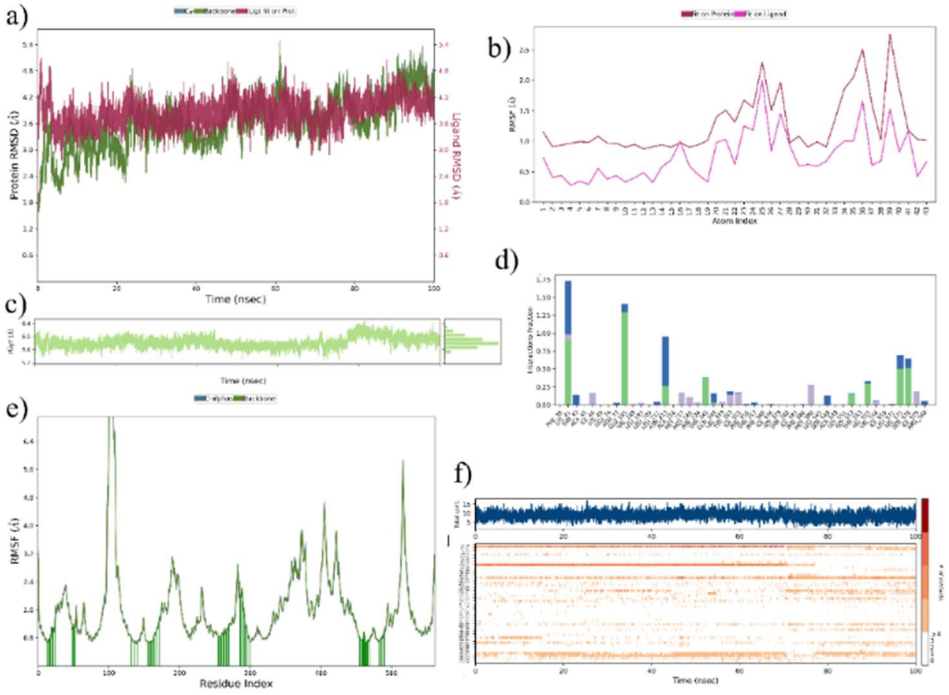

3.5 Drug-likeness, side Effects, and toxicity of HSP

HSP exhibited a favourable drug-likeness score (0.94), supporting its potential as a drug candidate. Although it exceeded several Lipinski's Rule of Five parameters, such deviations are common among bioactive flavonoids and do not necessarily limit therapeutic activity. The compound showed molecular weight of 610.19 (> 500) g/mol, low BBB permeability and a hydrophilic nature (MolLogP = −0.81). Toxicological assessment predicted non-carcinogenic and non-mutagenic properties, indicating a generally favourable safety profile. Environmental toxicity predictions suggested low aquatic toxicity. However, potential hERG inhibition was identified, warranting further investigation of cardiotoxicity risk. ADVERpred analysis indicated nephrotoxicity as the most probable adverse effect (Pa = 0.337; Pi = 0.124), consistent with reported renal sensitivity associated with certain glycosylated flavonoids.

4 DISCUSSION

An integrative in-silico systems pharmacology approach was used in this study to elucidate the mechanisms by which HSP may reduce DIC. HSP was selected based on its previously reported anti-inflammatory, antioxidant, and hepatoprotective potentials [42]. It was further supported by emerging data suggesting its function in transporter modulation and bile-acid regulation. Identification of common molecular targets relevant to cholestatic pathophysiology was made possible by an interaction analysis between HSP-associated targets and DIC-related genes gathered from established databases and literature. Using topological settings like node degree and edge connectivity, Cytoscape was used for generating a compound-target-pathway network that made it easier to visualize functional connectivity and identify important regulatory nodes [25]. MDK and MD simulations investigated structural compatibility and binding stability with specific DIC-associated proteins, while simultaneously assessing drug-likeness, toxicity prediction, and adverse-effect evaluations described the compound's safety profile.

Key regulators of bile acid homeostasis, such as FXR, BSEP, OATP1B1, NTCP, and MRP2-transporters that collectively control hepatic bile acid flux-were clearly identified among the 31 overlapping targets [43]. Bile acid buildup, oxidative stress, mitochondrial dysfunction, and hepatocyte apoptosis are all triggered

upon their disruption, which is essential to the pathophysiology of DIC. Hub proteins AKT1, TNF, IL6, NFE2L2, and STAT3 were also identified in the PPI network built with STRING, which is consistent with their known functions in oxidative stress regulation, inflammatory signaling, and hepatocyte protection in cholestatic disease [44].

FXR emerged as the principal hub node, consistent with its role as master regulator of bile acid homeostasis. FXR activation reduces hepatic bile acid re-uptake by suppressing de novo bile acid synthesis, inducing canalicular efflux transporters BSEP and MRP2, and downregulating NTCP via the FXR-SHP-CYP7A1 axis. The FDA's approval of obeticholic acid (OCA) for primary biliary cholangitis highlights the clinical validation of this pathway [45]. HSP's function as an FXR activator is further supported by experimental evidence in HepaRG cells and an ANIT-induced mouse model, HSP increased fecal bile acid excretion and decreased hepatic accumulation while upregulating BSEP, MRP2, and NTCP while inhibiting synthesis enzymes CYP7A1 and CYP27A1 [17]. Thus, the FXR-specific structure found in the network analysis is both computationally and experimentally consistent with molecular biology.

MDK analysis verified the network predictions, revealing that HSP has an ideal binding affinity value that is -9.5 kcal/mol in relation to the FXR ligand-binding domain. Numerous hydrogen bonds and hydrophobic interactions with crucial residues Arg331, Glu334, and Gln263 previously linked to receptor activation and agonist recognition stabilized this interaction. This binding profile is in accordance with an agonistic or inhibitory FXR modulation mechanism that can increase transcription of downstream transporter genes [45]. Comparative docking against ursodeoxycholic acid (UDCA) showed that HSP had comparable or better binding affinities for both FXR and OATP1B1 [46], offering initial structural validation without suggesting pharmacological equivalency.

OATP1B1 (encoded by *SLCO1B1*) is a sodium-independent uptake transporter predominantly expressed on the basolateral membrane of hepatocytes. It mediates hepatic uptake of bile acids, bilirubin, steroid conjugates, thyroid hormones, and numerous drugs, thereby playing a critical role in bile acid homeostasis and enterohepatic circulation. OATP1B1 efficiently transports conjugated bile acids, with 3-sulfo-glycolithocholate exhibiting particularly high affinity, highlighting its importance in hepatic clearance. Studies using OATP1B1-overexpressing HEK293 cells have confirmed its broad substrate specificity and sodium-independent transport mechanism [47]. Impaired OATP1B1 function, resulting from genetic polymorphisms, reduced expression, or pharmacological inhibition, contributes to the accumulation of bile acids and conjugated bilirubin in circulation, a hallmark of cholestatic liver disease. Histological analyses of patients with primary biliary and hepatocellular disorders demonstrated an inverse relationship between OATP1B1 expression and serum bilirubin levels, with the greatest reduction observed in advanced cholestatic conditions, providing direct clinical evidence of its pathological significance [48]. Furthermore, OATP1B1 inhibition, often accompanied by BSEP suppression, has been identified as a key mechanistic risk factor for drug-induced cholestasis and increased severity of drug-induced liver injury. Consequently, regulatory agencies, including the FDA and EMA, require in vitro assessment of OATP1B1 inhibition during drug development due to its critical role in hepatic drug disposition and cholestatic risk evaluation [49].

According to this known background, the HSP docking results towards OATP1B1 (PDB ID: 8HNC; −7.9 kcal/mol) have significant interpretive weight. The binding process included hydrophobic contacts with Ser576, Lys41, and Ile353, residues positioned in or close to the main substrate-binding pocket found in the 2023 cryo-EM studies, as well as hydrogen bonding with His575, Glu185, Tyr352, and Thr357. Previous studies used cryo-EM to resolve OATP1B1 in multiple ligand-bound states, revealing a major substrate-binding pocket in the C-terminal transmembrane domain that accommodates bilirubin, estrone-3-sulfate, and the clinical drug simeprevir [50]. Similarly, another study identified the substrate-binding site within the C-terminal half of OATP1B1, with estrone-3-sulfate occupying a pocket whose shape and electrostatic character explain the transporter's preference for a variety of amphipathic organic anions [51]. Direct computational verification that HSP interacts with the functionally significant binding region of OATP1B1 is provided by the overlap between the computed contact residues of HSP, specifically Tyr352, Val189, and Ile353, and those lining the structurally characterized major pocket. As a class, flavonoids have demonstrated their ability to modulate OATP1B1. Previous research also demonstrated that Ginkgo biloba flavonoids (apigenin, kaempferol, quercetin) competitively inhibited OATP1B1-mediated uptake of sulfobromophthalein and atorvastatin in HEK293-OATP1B1 cells [52]. Eight compounds (including kaempferol, luteolin, and biochanin A) were found to be significant OATP1B1 inhibitors (>50% inhibition in OATP1B1-HEK293 cells) in a recent systematic evaluation of 99 flavonoids. It was also confirmed that these flavonoids decreased serum total bile acid levels

and hepatic bosentan concentrations in a bosentan-induced rat liver injury model, offering in vivo validation that OATP1B1 modulation by flavonoids leads to quantifiable hepatoprotective effects [53]. The polyphenolic flavanone core of HSP shares the hydrogen bond donor-acceptor profile and hydrophobic ring system that have been identified as pharmacophoric determinants of flavonoid–OATP1B1 interaction in published structure–activity relationship (SAR) analyses, despite the fact that it differs structurally from these flavonoids (it carries a rhamnoglucose disaccharide at C-7). Furthermore, IL-6-mediated STAT3 activation has been demonstrated to transcriptionally suppress SLCO1B1 during inflammatory cholestasis, and OATP1B1 activation is biologically regulated by FXR. Since TNF, and IL-6 are among the targets of HSP's network pharmacology profile, it is possible that HSP will restore OATP1B1 expression through both direct transporter interaction and inhibition of the cell-mediated transcriptional suppression that characterizes cholestatic disease states. HSP is conceptually positioned as a multi-modal OATP1B1 regulator by this dual modulation - direct structural activation and indirect transcriptional recovery, a theory that requires experimental validation.

The docking results were validated by MD simulations run for more than 100 ns. Following initial equilibration, the HSP-FXR and HSP-OATP1B1 complexes both attained stable RMSD profiles, indicating that HSP is structurally and energetically in harmony with the binding cavities of both proteins under appropriate conditions. Key intermolecular contacts, such as hydrophobic interactions with Val189 and Tyr352 in OATP1B1 and hydrogen bonds with Arg331 and Glu334 in FXR, persist throughout the simulation courses, which is consistent with the formation of stable ligand-protein complexes. These results are typical of polyphenolic ligands, which can sustain fruitful binding interactions in dynamic protein environments due to their conformational flexibility [54]. The docking and MD data together provide a structural rationale for the hypothesized pharmacological activity of HSP at hepatic transporter and nuclear receptor targets.

Network analysis revealed that HSP interacts with a wider range of targets related to oxidative stress and inflammatory signalling, including NFE2L2 (Nrf2), AKT1, TNF-α, IL-6, and other components of the MAPK cascade, in addition to bile acid transport. In DIC, intrahepatic bile acid accumulation sets off a chain reaction of mitochondrial dysfunction, reactive oxygen species (ROS) production, and proinflammatory cytokine amplification that sustains hepatocyte injury and promotes fibrogenic progression [55]. These connections have pathophysiological significance. The master transcriptional regulator of the cellular antioxidant response is NFE2L2/Nrf2. Glutathione peroxidase (GPx), superoxide dismutase (SOD), and heme oxygenase-1 (HO-1) are examples of cytoprotective enzymes that are expressed when oxidative stress occurs because Nrf2 translocates to the nucleus and activates the antioxidant response element (ARE) [56,57]. According to experimental research, HSP increases cellular antioxidant defense capacity and shields hepatocytes from oxidative damage by activating Nrf2/HO-1 signalling in hepatic cells via the ERK/Nrf2 pathway [58]. Recent reviews showing the co-regulatory interaction between FXR and Nrf2 in suppressing liver inflammatory disease have shown that this antioxidant axis is complementary to FXR activation [45,59].

The enrichment of inflammatory signalling pathways like PI3K-Akt, MAPK, and NF-κB among the identified targets further supports a multi-target anti-inflammatory role for HSP in DIC. Significant decreases in hepatic inflammation have been linked to the suppression of the NF-κB and MAPK pathways, particularly p38 and JNK, which are key mediators of cytokine production in cholestatic liver injury [55,60]. The pharmacology of salvianolic acid B, which prevented ANIT-induced cholestatic injury through synergistic regulation of bile acid transporters and suppression of NF-κB/IκB and MAPK inflammatory cascades (60), a pattern of multi-target activity mirroring that proposed here for HSP illustrates this mechanistic progress. Additionally, the PI3K/Akt pathway is essential for controlling oxidative stress and hepatocyte survival; AKT1 activation is linked to increased expression of antioxidant enzymes and defense against ROS-induced cell death [61]. According previous research, HSP-mediated inhibition of caspase-associated apoptosis in DILI models [62], the interaction of HSP with AKT1, as shown by network topology, suggests that its hepatoprotective activity may partially operate through activation of hepatocyte survival signalling.

HSP has favourable pharmacological properties, such as non-mutagenic and non-carcinogenic behaviour, according to in silico drug-likeness and toxicity assessments. Despite HSP's violation of some Lipinski's Rule of Five parameters, which is a common characteristic of glycosylated flavonoids due to their higher molecular weight and polar surface area, pharmacological activity is not always inhibited because many clinically relevant polyphenolic natural products share these physicochemical deviations [20,54]. The anticipated hERG inhibition potential of HSP, which increases the risk of QT interval

prolongation and related cardiotoxicity, is a concern that needs more research. Since computational hERG risk predictions are known to be sensitive to structural features like aromatic ring systems that are common to many flavonoids and do not always predict in vivo cardiac effects, this in silico signal should be interpreted cautiously [54]. However, before any claims can be supported, specific in vitro and in vivo cardiotoxicity assays will be required.

A major limitation of this study is its exclusively computational nature. Although the findings are supported by existing literature, experimental validation in established cholestasis models, including primary human hepatocytes, bile duct ligation, and ANIT-induced rodent models, is required. Mechanistic studies such as FXR reporter assays, Western blotting, and LC–MS-based bile acid profiling would further verify the predicted pharmacological effects. Another limitation is the poor oral bioavailability of hesperidin, resulting from low solubility, limited absorption, extensive metabolism, and efflux mechanisms. Advanced hepatocyte-targeted delivery systems, including liposomes, phytosomes, and lipid-based nanoparticles, may enhance its therapeutic potential and warrant further investigation [63-65].

5 CONCLUSION

In conclusion, the current integrative computational studies support HSP's hepatoprotective potential in DIC. The substance is speculated to use a coordinated multi-target pharmacological approach that includes activation of Nrf2-dependent antioxidant defenses, suppression of NF-κB/MAPK-driven inflammatory signaling, modulation of hepatocellular bile acid transport via OATP1B1, and transcriptional regulation of bile acid metabolism via FXR. The complex, systems-level nature of cholestatic liver injury is reflected in this multi-axis mode of action, where the entire pathological range cannot be explained by a single molecular event. HSP is intended as a promising lead molecule for additional preclinical development against DIC in liver disease due to its established safety profile, the structural compatibility and dynamic stability of HSP interactions with FXR and OATP1B1 as suggested by MDK and MD simulation, and the availability of its bioavailability limitations through nanotechnology.

AUTHOR CONTRIBUTIONS

All the authors contributed significantly to the article's conception and design, data collection, analysis, and interpretation, participated in its drafting or critical revision for significant intellectual content, consented to submit it to the current journal, approved the final version for publication, and agreed to take full responsibility for the work. According to the rules and regulations set forth by the International Committee of Medical Journal Editors (ICMJE), each author is qualified to be an author.

LIST OF ABBREVATIONS

BE: Binding energy; DLS: Drug-likeness score; HBI: Hydrogen-bond interactions; NHBI: Non-hydrogen-bond interactions; NP: Network Pharmacology; PPI: Protein-Protein Interaction; MDK: Molecular Docking; MD: Molecular dynamics; RMSD: Root-mean-square deviation; RMSF: Root-mean-square fluctuation; rGyr: Radius of gyration; SPC: Simple point charge; MMFF94: Merck molecular force field 94; FXR: Farnesoid X receptor; OATP1B1: Organic anion transporting polypeptide 1B1; DIC: Drug-induced cholestasis; DILI: Drug-induced liver injury; HSP: Hesperidin; KEGG: Kyoto Encyclopedia of Genes and Genomes; CTD: Comparative Toxicogenomics Database; BBB: Blood–brain barrier; ARE: Antioxidant response element; Pa: Probability of activity; Pi: Probability of inactivity; LC50: Lethal concentration 50%.

FINANCIAL SUPPORT

There is no funding to report.

CONFLICTS OF INTEREST

The authors disclose no financial or other conflicts of interest.

AI TOOL DISCLOSURE

This manuscript utilized AI generative tool ChatGPT solely for grammar correction and language refinement.

ETHICAL APPROVALS

There are no human or animal trials involved in this study.

DATA AVAILABILITY

The information supporting the study's conclusions is accessible upon reasonable request.

REFERENCES

1. Asensio M, Ortiz-Rivero S, Morente-Carrasco A, Marin JJG. Etiopathogenesis and pathophysiology of cholestasis. *Explor Dig Dis.* 2022;1:97–117.
2. Ommati MM, Attari H, Siavashpour A, Shafaghat M, Azarpira N, Ghaffari H, *et al*. Mitigation of cholestasis-associated hepatic and renal injury by edaravone treatment: evaluation of its effects on oxidative stress and mitochondrial function. *Liver Res.* 2021;5(3):181–193.

3. Grant LM, John S. Cholestatic jaundice. In: StatPearls [Internet]. Treasure Island (FL): StatPearls Publishing; 2025. Available from: http://www.ncbi.nlm.nih.gov/books/NBK482279/
4. Pinazo-Bandera JM, Toro-Ortiz JP, Andrade RJ, García-Cortés M. Drug-induced cholestasis: causative agents and challenges in diagnosis and management. *Explor Dig Dis.* 2023;2(5):202–222.
5. Kolarić TO, Ninčević V, Smolić R, Smolić M, Wu GY. Mechanisms of hepatic cholestatic drug injury. *J Clin Transl Hepatol.* 2019;7:1–7.
6. Pedersen JM, Matsson P, Bergström CAS, Hoogstraate J, Norén A, LeCluyse EL, *et al*. Early identification of clinically relevant drug interactions with the human bile salt export pump (BSEP/ABCB11). *Toxicol Sci.* 2013;136(2):328–343.
7. Kong B, Wang L, Chiang JYL, Zhang Y, Klaassen CD, Guo GL. Mechanism of tissue-specific farnesoid X receptor in suppressing the expression of genes in bile-acid synthesis in mice. *Hepatology.* 2012;56(3):1034–1043.
8. Matsubara T, Li F, Gonzalez FJ. FXR signaling in the enterohepatic system. *Mol Cell Endocrinol.* 2013;368(1):17–29.
9. Li T, Chiang JYL. Nuclear receptors in bile acid metabolism. *Drug Metab Rev.* 2013;45(1):145–155.
10. Robles-Díaz M, Nezic L, Vujic-Aleksic V, Björnsson ES. Role of ursodeoxycholic acid in treating and preventing idiosyncratic drug-induced liver injury: a systematic review. *Front Pharmacol.* 2021;12.
11. Buechter M, Manka P, Bulut K, Gerken G, Kahraman A. Obeticholic acid improves cholestasis, liver fibrosis, and liver function in patients with primary biliary cholangitis with inadequate response to ursodeoxycholic acid. *J Pers Med.* 2025;15(3):79.
12. D'Amato D, De Vincentis A, Malinverno F, Viganò M, Alvaro D, Pompili M, *et al*. Real-world experience with obeticholic acid in patients with primary biliary cholangitis. *JHEP Rep.* 2021;3(2):100248.
13. Gajender, Mazumder A, Sharma A, Azad AK. A comprehensive review of the pharmacological importance of dietary flavonoids as hepatoprotective agents. *Evid Based Complement Altern Med.* 2023;2023:4139117.
14. Jomova K, Alomar SY, Valko R, Liska J, Nepovimova E, Kuca K, *et al*. Flavonoids and their role in oxidative stress, inflammation, and human diseases. *Chem Biol Interact.* 2025;413:111489.
15. Nasehi Z, Kheiripour N, Akhavan Taheri M, Ardjmand A, Jozi F, Shahaboddin ME. Efficiency of hesperidin against liver fibrosis induced by bile duct ligation in rats. *Biomed Res Int.* 2023;2023:5444301.
16. Li Y, Kandhare AD, Mukherjee AA, Bodhankar SL. Acute and sub-chronic oral toxicity studies of hesperidin isolated from orange peel extract in Sprague Dawley rats. *Regul Toxicol Pharmacol.* 2019;105:77–85.
17. Zhang G, Sun X, Wen Y, Shi A, Zhang J, Wei Y, *et al*. Hesperidin alleviates cholestasis via activation of the farnesoid X receptor in vitro and in vivo. *Eur J Pharmacol.* 2020;885:173498.
18. Harakeh S, Niyazi HA, Niyazi HA, Abdalal SA, Mokhtar JA, Almuhayawi MS, *et al*. Integrated network pharmacology approach to evaluate bioactive phytochemicals of Acalypha indica and their mechanistic actions to suppress target genes of tuberculosis. *ACS Omega.* 2024;9(2):2204–2219.
19. Mazri R, Ouassaf M, Zekri A, Khan SU, Rengasamy KRR, Alhatlani BY. In silico network pharmacology, molecular docking, and molecular dynamics analysis of rosemary-derived compounds as potential HSP90 inhibitors for cancer therapy. *Curr Issues Mol Biol.* 2025;47(10):860.
20. Tabeshpour J, Hosseinzadeh H, Hashemzaei M, Karimi G. A review of the hepatoprotective effects of hesperidin, a flavanone glycoside in citrus fruits, against natural and chemical toxicities. *DARU J Pharm Sci.* 2020;28(1):305–317.
21. Patil VS, Harish DR, Vetrivel U, Roy S, Deshpande SH, Hegde HV. Hepatitis C virus NS3/4A inhibition and host immunomodulation

by tannins from Terminalia chebula: a structural perspective. *Molecules.* 2022;27(3):1076.
22. Stelzer G, Rosen N, Plaschkes I, Zimmerman S, Twik M, Fishilevich S, *et al*. The GeneCards suite: from gene data mining to disease genome sequence analyses. *Curr Protoc Bioinformatics.* 2016;54(1):1.30.1–1.30.33.
23. Liu B, Zhang J, Shao L, Yao J. Network pharmacology analysis and molecular docking to unveil the potential mechanisms of San-Huang-Chai-Zhu formula treating cholestasis. *PLoS One.* 2022;17(2):e0264398.
24. Beerwala FA, Kolambkar SV, Karikazi A, Khatib NA, Bhandare VV, Roy S, *et al*. Harnessing the therapeutic potential of Garcinia indica Choisy constituents against olanzapine-induced cardiac and metabolic disorders. *In Silico Res Biomed.* 2025;1:100010.
25. Shannon P, Markiel A, Ozier O, Baliga NS, Wang JT, Ramage D, *et al*. Cytoscape: a software environment for integrated models of biomolecular interaction networks. *Genome Res.* 2003;13(11):2498–2504.
26. Alos HC, Billones JB, Castillo AL, Vasquez RD. Alpinumisoflavone against cancer pro-angiogenic targets: in silico, in vitro, and in ovo evaluation. *DARU J Pharm Sci.* 2022;30:273–288.
27. Trott O, Olson AJ. AutoDock Vina: improving the speed and accuracy of docking with a new scoring function, efficient optimization, and multithreading. *J Comput Chem.* 2010;31(2):455–461.
28. Kandhwal M, Grewal AK, Singh M, Singh M, Singh V, Singh TG. Neuroprotective effects of hesperidin: in-vitro and in silico evaluation of its antioxidant and enzyme inhibitory activities. *Carpathian J Food Sci Technol.* 2024;16(4):188.
29. Dawuti A, Ma L, An X, *et al*. Exploring the effect and mechanism of Aloin A against cancer cachexia-induced muscle atrophy via network pharmacology, molecular docking, molecular dynamics and experimental validation. *Aging (Albany NY).* 2023;15(24):15557–15577.
30. Jendele L, Krivak R, Skoda P, Guan J, Zhou C, He L, *et al*. PrankWeb: a web server for ligand binding site prediction and visualization. *Nucleic Acids Res.* 2019;47(W1):W345–W349.
31. Harish D, Patil V, Roy S. In silico studies in predicting mechanism of action of Amaranthus tricolor on Alzheimer's disease. *Indian J Pharm Sci.* 2022;84(2):328–340.
32. Ugare SR, Khatib NA, Patil VS, Patil D, Dodakallanavar J. Computational and experimental pharmacology reveals hepatoprotective effect of Cucurbita pepo in isoniazid-induced liver cirrhosis. *J Appl Pharm Sci.* 2024;14(1):177–188.
33. Fatriansyah JF, Rizqillah RK, Yandi MY. Molecular docking and molecular dynamics simulation of fisetin, galangin, hesperetin, hesperidin, myricetin, and naringenin against polymerase of dengue virus. *J Trop Med.* 2022;2022:7254990.
34. Ivanov SM, Lagunin AA, Rudik AV, Filimonov DA, Poroikov VV. ADVERPred - web service for prediction of adverse effects of drugs. *J Chem Inf Model.* 2018;58(1):8–11.
35. Kumar V, Sharma N, Orfali R, Patel CN, Alnajjar R, Saini R, *et al*. Multitarget potential of phytochemicals from Terminalia arjuna (Roxb. ex DC.) Wight & Arn. as potential medicaments for cardiovascular disease: an in silico approach. *Molecules.* 2023;28(3):1046.
36. Vatakuti S, Pennings JLA, Gore E, Olinga P, Groothuis GMM. Classification of cholestatic and necrotic hepatotoxicants using transcriptomics on human precision-cut liver slices. *Chem Res Toxicol.* 2016;29(3):342–351.
37. Roman DL, Roman M, Som C, Schmutz M, Hernandez E, Wick P, *et al*. Computational assessment of the pharmacological profiles of degradation products of chitosan. *Front Bioeng Biotechnol.* 2019;7:214.
38. Atta IS, Elnady MR, Alghamdi AG, Alghamdid AH, Aboulata AA, Shatla IM. Assessing the hepatoprotective effects of hesperidin on liver-associated disorders in albino rats with experimentally induced obesity and type II diabetes: a histological and biochemical study. *Heliyon.* 2023;9(5):e16031.
39. Desaipatti R, Kudatarkar N, Gudasi S. In silico screening and experimental validation of Carissa

carandas L. extract against cyclophosphamide-induced cardiotoxicity in Wistar rats. *J Appl Pharm Sci.* 2025;15(3):1–10.

40. Patil VS, Patil CR, Patel HM, Kumar A. Exploring disulfiram mechanisms in renal fibrosis: insights from biological data and computational approaches. *Front Pharmacol.* 2025;16:1480732.
41. Hospital A, Goñi JR, Orozco M, Gelpí JL. Molecular dynamics simulations: advances and applications. *Adv Appl Bioinform Chem.* 2015;8:37–47.
42. Morshedzadeh N, Ramezani Ahmadi A, Behrouz V, Mir E. A narrative review on the role of hesperidin on metabolic parameters, liver enzymes, and inflammatory markers in nonalcoholic fatty liver disease. *Food Sci Nutr.* 2023;11(12):7523–7533.
43. Tveter KM, Mezhibovsky E, Wu Y, Roopchand DE. Bile acid metabolism and signaling: emerging pharmacological targets of dietary polyphenols. *Pharmacol Ther.* 2023;248:108457.
44. Wang Y, Tan N, Su R, Lui Z, Hu N, Dong Q. Exploring the potential mechanisms of action of Gentiana veitchiorum Hemsl. extract in the treatment of cholestasis using UPLC-MS/MS, systematic network pharmacology, and molecular docking. *Comb Chem High Throughput Screen.* 2024;27(13):1948–1968.
45. Kim I, Ahn SH, Inagaki T, Choi M, Ito S, Guo GL, *et al*. Differential regulation of bile acid homeostasis by the farnesoid X receptor in liver and intestine. *J Lipid Res.* 2007;48(12):2664–2672.
46. Bessone F, Hillotte GL, Tamagnone N, Arnedillo D, Roma MG. Ursodeoxycholic acid for the management of drug-induced liver injury: role of hepatoprotective and anti-cholestatic mechanisms. *J Clin Transl Hepatol.* 2025;13(2):162–168.
47. Tóth B, Jani M, Beéry E, Heslop T, Bayliss M, Kitteringham NR, et al. Human OATP1B1 (SLCO1B1) transports sulfated bile acids and bile salts with particular efficiency. Toxicol In Vitro. 2018;52:189–194
48. Sticova E, Lodererova A, van de Steeg E, Frankova S, Kollar M, Lanska V, et al. Down-regulation of OATP1B proteins correlates with hyperbilirubinemia in advanced cholestasis. Int J Clin Exp Pathol. 2015;8(5):5252–5262.
49. Kotsampasakou E, Brenner S, Jäger W, Ecker GF. Identification of novel inhibitors of organic anion transporting polypeptides 1B1 and 1B3 (OATP1B1 and OATP1B3) using a consensus vote of six classification models. Mol Pharm. 2015;12(12):4395–4404
50. Shan Z, Yang X, Liu H, Yuan Y, Xiao Y, Nan J, et al. Cryo-EM structures of human organic anion transporting polypeptide OATP1B1. Cell Res. 2023;33(12):940–951
51. Ciută AD, Nosol K, Kowal J, Mukherjee S, Ramírez AS, Stieger B, et al. Structure of human drug transporters OATP1B1 and OATP1B3. Nat Commun. 2023;14(1):5774.
52. Mandery K, Balk B, Bujok K, Schmidt I, Fromm MF, Glaeser H. Inhibition of hepatic uptake transporters by flavonoids. Eur J Pharm Sci. 2012;46(1–2):79–85
53. Fan X, Bai J, Hu M, Xu Y, Zhao S, Sun Y, et al. Drug interaction study of flavonoids toward OATP1B1 and their 3D structure activity relationship analysis for predicting hepatoprotective effects. Toxicology. 2020;437:152445
54. Donia T, Dabbour NM, Loutfy SA. Hesperidin: advances on resources, biosynthesis pathway, bioavailability, bioactivity, and pharmacology. In: Handbook of Dietary Flavonoids. Cham: Springer; 2023. p. 1–55.
55. Xiang D, Yang J, Xu Y, Lan L, Li G, Zhang C, *et al*. Estrogen cholestasis induces gut and liver injury in rats involving activation of PI3K/Akt

and MAPK signaling pathways. *Life Sci.* 2021;276:119367.

56. Huang W, Zhong Y, Gao B, Zheng B, Lu Y. Nrf2-mediated therapeutic effects of dietary flavones in different diseases. *Front Pharmacol.* 2023;14:1240433.
57. Chen M, Ye Y, Ji G, Liu J. Hesperidin upregulates heme oxygenase-1 to attenuate hydrogen peroxide-induced cell damage in hepatic L02 cells. *J Agric Food Chem.* 2010;58(6):3330–3335.
58. Huang Q, Liu J, Peng C, Han X, Tan Z. Hesperidin ameliorates H2O2-induced bovine mammary epithelial cell oxidative stress via the Nrf2 signaling pathway. *J Anim Sci Biotechnol.* 2024;15(1):57.
59. Belka M, Gostyńska-Stawna A, Stawny M, Krajka-Kuźniak V. Activation of Nrf2 and FXR via natural compounds in liver inflammatory disease. *Int J Mol Sci.* 2024;25(20):11213.
60. Li S, Wang R, Wu B, Wang Y, Song F, Gu Y, *et al*. Salvianolic acid B protects against ANIT-induced cholestatic liver injury through regulating bile acid transporters and enzymes, and NF-κB/IκB and MAPK pathways. *Naunyn Schmiedebergs Arch Pharmacol.* 2019;392(9):1169–1180.

.

61. Shamsan E, Almezgagi M, Gamah M, Khan N, Qasem A, Chuanchuan L, *et al*. The role of PI3K/AKT signaling pathway in attenuating liver fibrosis: a comprehensive review. *Front Med.* 2024;11:1389329.
62. Gur C, Kandemir FM, Caglayan C, Satici E. Chemopreventive effects of hesperidin against paclitaxel-induced hepatotoxicity and nephrotoxicity via amendment of Nrf2/HO-1 and caspase-3/Bax/Bcl-2 signaling pathways. *Chem Biol Interact.* 2022;365:110073.
63. Wdowiak K, Walkowiak J, Pietrzak R, Bazan-Woźniak A, Cielecka-Piontek J. Bioavailability of hesperidin and its aglycone hesperetin — compounds found in citrus fruits as a parameter conditioning the pro-health potential (neuroprotective and antidiabetic activity) — mini-review. *Nutrients.* 2022;14(13):2647.
64. Hoang TPN, Timmins P, Smith AM, Conway BR, Ghori MU. Drug delivery and formulation development of hesperidin: a systematic review. *Expert Opin Drug Deliv.* 2026;23(2):363–384.
65. D'Souza AA, Devarajan PV. Asialoglycoprotein receptor mediated hepatocyte targeting: strategies and applications. *J Control Release.* 2015;203:126–139.